

Article

Optimized Fuzzy Logic Control System for Diver's Automatic Buoyancy Control Device

Nenad Muškinja * , Matej Rižnar and Marjan Golob 

Faculty of Electrical Engineering and Computer Science, University of Maribor, SI-2000 Maribor, Slovenia

* Correspondence: nenad.muskinja@um.si; Tel.: +386-2-220-7162

Abstract: In this article, the design of a fuzzy logic control system (FLCS) in combination with multi-objective optimization for diver's buoyancy control device (BCD) is presented. To either change or maintain the depth, the diver manually controls two pneumatic valves that are mounted on the inflatable diving jacket. This task can be very difficult, especially in specific diving circumstances such as poor visibility, safety stop procedures or critical life functions of the diver. The implemented BCD hardware automatically controls the diver's depth by inflating or deflating the diver's jacket with two electro-pneumatic valves. The FLCS in combination with the multi-objective optimization was used to minimize control error and simultaneously ensure minimal air supply consumption of the BCD. The diver's vertical velocity is also critical, especially while the diver is ascending during the decompression procedure; therefore, a combination of depth and vertical velocity control was configured as a cascaded controller setup with outer proportional depth and inner FLCS vertical velocity control loops. The optimization of the FLCS parameters was achieved with differential evolution global optimum search algorithm. The results obtained were compared with the optimized cascaded position and velocity PID controller in simulations.

Keywords: buoyancy control device; differential evolution optimization; fuzzy logic control system; nonlinear system control; position and velocity control

MSC: 93-10; 93B12; 93B51; 93B52



Citation: Muškinja, N.; Rižnar, M.; Golob, M. Optimized Fuzzy Logic Control System for Diver's Automatic Buoyancy Control Device. *Mathematics* **2023**, *11*, 22. <https://doi.org/10.3390/math11010022>

Academic Editor: Asier Ibeas

Received: 5 December 2022

Revised: 18 December 2022

Accepted: 19 December 2022

Published: 21 December 2022



Copyright: © 2022 by the authors. Licensee MDPI, Basel, Switzerland. This article is an open access article distributed under the terms and conditions of the Creative Commons Attribution (CC BY) license (<https://creativecommons.org/licenses/by/4.0/>).

1. Introduction

The most recent research on wearables for underwater use presents a comprehensive map of their performance and characteristics, discussing the general direction of the development of underwater wearables and the direction of research towards new prototypes [1]. The safety devices seem to have gained the most interest at the time of this study [2–4]. One of the proposed automatic system is a patented electronic device pluggable on standard over pressure valves of scuba jackets aimed at detecting the occurrence of too fast, possibly uncontrolled, ascents of the diver [5]. In this work, authors have proposed, designed and tested an actuated venting valve for an innovative wearable anti rapid ascent system. Until now, no commercial automatic diver buoyancy control system has yet been developed. Much more research has been devoted to the automatic control of an autonomous underwater vehicles (AUVs). The depth control of the floating ocean seismograph considers the variation of seawater density with depth [6]. This work mainly focuses on the design of a self-adaptive fuzzy PID controller. Design of controllers for underwater vehicles is challenging due to their nonlinear dynamics, time-varying model parameters, and environmental disturbances, which are difficult to measure or estimate. The next article describes a hybrid depth controller for a standalone variable buoyancy (VB) engines [7]. Individual controllers, such as PID, LQR, and SMC, were developed after mathematically modeling the dynamics of the module and its actuator. A comprehensive review of underwater gliding robots, including prototype design and their key technologies, is very well described in [8].

There are several types of diving jackets that are used for scuba diving. These include:

1. BC (Buoyancy Control) jacket: This is the most common type of diving jacket and is worn by most scuba divers. It is designed to help the diver control their buoyancy while underwater by adding or releasing air from a built-in bladder.
2. Wing jacket: This type of diving jacket is similar to a BC jacket, but it has a larger, wing-shaped bladder that wraps around the diver's sides and back. This design allows the diver to carry more air, which can be useful for deeper dives or longer bottom times.
3. Drysuit: A drysuit is a type of diving jacket that is designed to keep the diver's body completely dry while diving. It is made of a waterproof and breathable material and is sealed at the wrists, ankles, and neck to prevent water from entering. Drysuits are typically worn in colder water or when the diver wants to stay dry for extended periods of time.
4. Wetsuit: A wetsuit is a type of diving jacket that is made of neoprene and is worn to keep the diver warm while diving in cold water. It is not designed to keep the diver completely dry, but rather to trap a thin layer of water between the wetsuit and the diver's skin, which is heated by the body and helps to keep the diver warm.
5. Rash guard: A rash guard is a type of diving jacket that is worn over a swimsuit or wetsuit to provide additional sun protection and to prevent chafing. It is made of a stretchy, moisture-wicking material and is often worn by surfers and other water sports enthusiasts.

Divers mostly use flexible BCDs, so we will only focus on them in this paper. An automatic depth control of the diver can be achieved with electrically driven pneumatic valves. Many existing solutions have been introduced [9–14], but so far no commercial product on the diver market provides automatic diver depth and vertical velocity control. An efficient automatic BCD is therefore still a major challenge to be solved.

For effective automatic control of the BCD, three control objectives must be considered, namely depth, vertical velocity, and minimal air consumption. The most critical objective for a diver's health is correct decompression during ascent to the surface [15].

Controlling the diver depth and the vertical velocity is difficult due to the compressibility of the BCD and the nonlinearity of the volume flows of the pneumatic valves. As the diver descends (ascends), the air in the BCD is compressed (decompressed). This causes additional acceleration of the diver. The pressure in the BCD and the volumetric flows of the inflation and deflation valves also change with depth and must be compensated by the manual or automatic control of the inflation and deflation valves. The nonlinearities of the volume flows of the pneumatic valves, the compressibility of the BCD and the vertical movement of the divider are presented in detail in [16]. A detailed dynamic model of a diver with all accessories is proposed in [17]. In particular, the design of a mathematical model of diver buoyancy, the BCD, and pneumatic valves is presented. The nonlinearities of the BCDs' volume with respect to the diver depth are considered and the nonlinearities of the volumetric flow of the pneumatic valves with respect to the depth and volume of the BCDs are analyzed. The effectiveness of the proposed model was validated by comparing the simulation results with the measurement results of various experiments.

In our previous work [18], the optimized diving and depth control for the diver's automatic BCD used computer-aided optimization of a cascaded controller setup with outer depth proportional and inner linear PID vertical velocity control loops. During the controller optimization, process optimized controller parameters were obtained in the simulation environment on the buoyancy dynamics model and compared with the manually driven BCD.

Figure 1 shows a modern type of the diver's buoyancy control device (BCD). Two pneumatic valves inflate or deflate the air-filled jacket and consequently ascend or descend the BCD.



Figure 1. Modern type of the buoyancy control device or BCD.

An experienced diver can reach the desired depth with minimal consumption of compressed air from the diver's gas cylinder. Using the inflation and deflation valves in combination with correct breathing, the diver can control the vertical velocity of ascent or descent and the depth at the same time. Major problems can arise in exceptional circumstances, such as pure visibility, safety stop procedures or critical life functions of the diver. In such situations, the use of an automated control system for BCD would be very significant.

The use of the most popular linear PID controller may not perform satisfactorily in the presence of nonlinearities and uncertainties in the real control system. Therefore, a variable gain nonlinear controller such as fuzzy PID (FPID) can be one of the possible solutions.

The use of fuzzy logic controller (FLC) in nonlinear control systems has proven to be one of the best solutions for transferring the expert knowledge of operators to the control algorithm. A successfully controlled steam engine was the very first practical implementation of FLC [19]. A Mamdani type of fuzzy PI controller [20] has been a very important shift in fuzzy control theory. Many T1FPID control strategies can be found [21–23]. The simplest T1FPID controllers [24–26] showed significant performance improvement over the linear PID controllers when implemented in real time on an unstable nonlinear plant.

In this paper, a nonlinear FPID controller has been used in two different control strategies. The simple direct FPID controller was first tested in simulations on an existing nonlinear BCD mathematical model. The result was oscillating depth control around the depth reference trajectory and a vertical velocity of the diver that exceeds the safety requirements for the diver. The improvement of the simple direct FPID controller was performed using a global optimum search algorithm with differential evolution. Oscillations around the reference depth still occurred, the vertical velocity exceeded the safety requirements, and the air consumption was very high. A significant improvement was achieved by changing the structure of the control system. The FPID controller was configured as a velocity controller in the inner control loop and the linear proportional depth controller in the outer control loop. To optimize the closed-loop control requirements, the global optimum search algorithm with differential evolution was again applied. The final and best result was achieved with a cascaded P-FPID controller structure, which fulfilled all the control requirements with reduced final air consumption.

The main contributions of this work are:

1. New optimized fuzzy logic PID methodologies for solving the multi-objective control problem for the automatic BCD model.
2. New cascaded nonlinear P-FPID controller structure.
3. Application of a global optimal search algorithm of differential evolution with three different objective functions to improve the BCD control results.
4. The automatic BCD with cascaded optimized P-FPID controller achieved a 30% reduction in air consumption, which can be a major advantage in critical diving situations.
5. The thesis that a nonlinear variable gain controller such as Fuzzy PID can perform better than a linear PID controller in the presence of nonlinearities and uncertainties in a real control system is confirmed.

After a brief introduction, the article is organized as follows. In Section 2, the problem is formulated and a mathematical model of the dynamics of diver buoyancy and the dynamics of BCD is described, together with the dynamics of the inflation and deflation valves, and all assumptions and simplifications for testing the BCD in simulations. Section 3 describes the design, structure, and simulation results of the implemented simple depth (position) fuzzy PD control system. In Section 4, optimization-aided design for three different working regimes (objective functions) is described. In addition, the design, structure, and simulation results of the optimized position fuzzy PD and optimized cascaded P-FPID controller for BCD depth and disturbance control is analyzed and compared with the linear P-PID diver's depth controller. Finally, all conclusions and remarks are presented in Section 5.

2. Problem Formulation

Successful control of a diver's depth requires a good understanding of the dynamic behavior of the system. A mathematical model of diver's buoyancy derived in [17] describes a vertical movement of the diver's depth z , diver's vertical velocity \dot{z} and diver's vertical acceleration \ddot{z} :

$$m_d \ddot{z}(t) = m_d \cdot g - \rho_w \cdot g[V_{BCD}(t) + V_d] - \frac{1}{2} \cdot \rho_w \cdot c_d \cdot |\dot{z}(t)| \cdot \dot{z}(t) \cdot [S_{BCD} + S_d], \quad (1)$$

where m_d is diver mass with equipment, ρ_w is water density, V_{BCD} and S_{BCD} are the buoyancy device volume and cross-section, V_d and S_d are the diver's volume and cross-section, c_d is the drag parameter and g is the gravitational constant.

The BCD's volume $V_{BCD}(t)$ is a BCD control parameter, where cross-section of the BCD S_{BCD} varies with the depth of the BCD. The neutral buoyancy of the diver at all depths can be derived from Equation (1).

To model a BCD's dynamic, we must consider that the air inside the BCD expands or contracts depending on the surrounding pressure $p_z(t)$:

$$\frac{p_z(t) \cdot V_{BCD}(t)}{T_z(t)} = \frac{p_z(0) \cdot V_{BCD}(0)}{T_z(0)} + \psi(t), \quad (2)$$

where the BCD's volume $V_{BCD}(t)$ depends on the initial BCD volume $V_{BCD}(0)$, the initial depth $z(0)$, the initial temperature $T_z(0)$ and the sum of the inflated/deflated volume $\psi(t)$.

If we assume that a BCD's volume $V_{BCD}(t)$ is controlled by two electro-pneumatic valves, then the control signal u has three states:

$$u = \begin{cases} 1 & add \\ 0 & none \\ -1 & deduct \end{cases}, \quad (3)$$

and the inflated/deflated volume $\psi(t)$ is then:

$$\psi(t) = \begin{cases} \frac{p_z(t)}{T_{aI}(t)} \int_{\tau=0}^t q_{VI}(\tau) \cdot d\tau & u = 1 \\ 0 & u = 0 \\ -\frac{p_z(t)}{T_{aD}(t)} \int_{\tau=0}^t q_{VD}(\tau) \cdot d\tau & u = -1 \end{cases}, \quad (4)$$

$$p_z(t) = \rho_w \cdot g \cdot z(t) + p_0 \quad (5)$$

where $p_z(t)$ is the surrounding pressure at depth $z(t)$, p_0 is the pressure at the water surface, $T_{aI}(t)$ is the absolute inflated air temperature, $T_{aD}(t)$ is the absolute deflated air temperature, $q_{VI}(\tau)$ is the added valve volume flow, and q_{VD} is the deducted valve volume flow.

All this leads to a BCD model:

$$V_{BCD}(t) = T_z(t) \left[\frac{1}{T_z(0)} \frac{(\rho_w \cdot g \cdot z(0) + p_0) \cdot V_{BCD}(0)}{\rho_w \cdot g \cdot z(t) + p_0} + \psi(t) \right], \quad (6)$$

$$\psi(t) = \begin{cases} \frac{1}{T_{aI}(t)} \int_{\tau=0}^t q_{VI}(\tau) \cdot d\tau & u = 1 \\ 0 & u = 0 \\ -\frac{1}{T_{aD}(t)} \int_{\tau=0}^t q_{VD}(\tau) \cdot d\tau & u = -1 \end{cases}. \quad (7)$$

An inflate valve volume flow model derived from [9] is:

$$q_{VI}(t) = \frac{\alpha_I \cdot A_I \cdot (\rho_w \cdot g \cdot z(t) + p_0 + p_r) \sqrt{R_a \cdot T_{aI}(t) \cdot \kappa \cdot \left[\frac{2}{(\kappa+1)} \right]^{\frac{(\kappa+1)}{(\kappa-1)}}}}{\rho_w \cdot g \cdot z(t) + p_0}, \quad (8)$$

where α_I considers the inflate valve orifice's shape, A_I is the inflate valve orifice area, p_r is the pressure of the diving regulator, κ is the fluid type dependent constant and R_a is the air gas constant.

At the end a deflate valve volume flow model is:

$$q_{VD}(t) = \alpha_D A_D \sqrt{\frac{2 \cdot R_a \cdot T_{aD}(t) \cdot \rho_w \cdot g \cdot \left(\frac{V_{BCD}(t)}{S_{BCD}} \right)}{\rho_w \cdot g \cdot z(t) + p_0}}, \quad (9)$$

where α_D considers the deflate valve orifice's shape and A_D is the deflate valve orifice area.

Based on the derived nonlinear mathematical model of BCD, a Matlab–Simulink simulation model was developed. Figure 2 shows the Matlab–Simulink schematic, which consists of sub-models for the inflation valve, deflation valve, BCD volume, drag force, buoyancy force, gravity force and a sub-model for the calculation of the BCD depth and velocity.

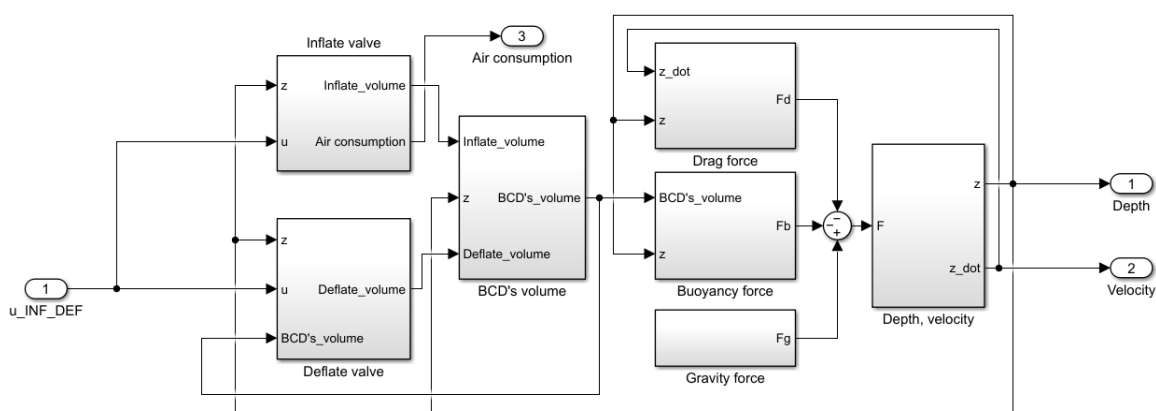


Figure 2. Matlab–Simulink model of a diver's buoyancy.

Several diving experiments were carried out to test the mathematical model. The derived mathematical model of diver buoyancy can be used to develop and test different depth control algorithms for automatic diver buoyancy control. Simulations and measurements are limited to vertical motion and a fixed vertical position of the diver, so the frontal air surface of the diver is considered constant. All other variables are assumed to be measurable. The proposed mathematical model is also applicable to other applications using flexible buoyancy tanks and pneumatic valves.

A summary of the symbolic parameters and simulation values are shown in Table A1 in the Appendix A.

3. Fuzzy Logic Control System Setup

Fuzzy logic control systems (FLCS) offer a wide range of implementation options, especially for controlling highly complex nonlinear processes. The design and structure of FLCS often depend on the intuition of the designer and the knowledge of the operator. In combination with an optimization mechanism, FLCS may improve an optimally designed linear controller due to their nonlinear behavior with multiple inputs and multiple outputs.

To improve the previously optimized cascaded depth and vertical velocity controller [18], a new control scheme is proposed. We started with a simple fuzzy PD scheme (Figure 3), where the diver's depth position error e_p is defined as the difference between the desired depth z_{ref} and the actual depth z :

$$e_p = z_{ref} - z, \quad (10)$$

and the diver's vertical change of depth over time or ascending and descending velocity dz/dt are inputs of the FLCS. The output u of the FLCS is inflating or deflating action of the electro-pneumatic BCD valves.

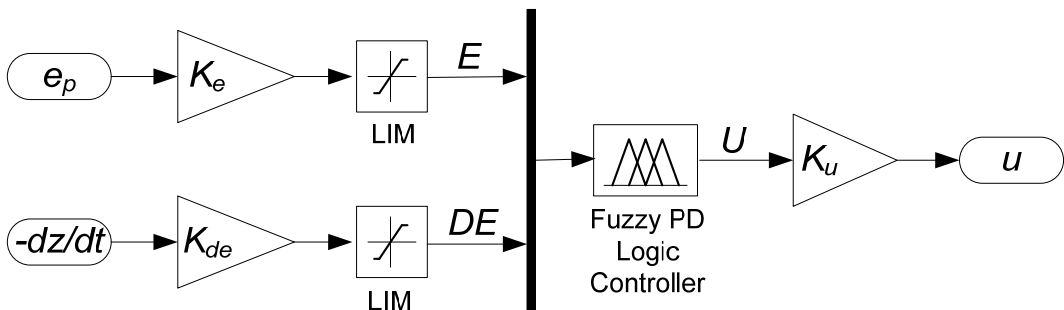


Figure 3. Fuzzy PD logic controller setup.

Fuzzy PD input signal gains K_e and K_{de} are used to fit the position error e_p and the diver's vertical change of depth over time dz/dt into the normalized definition space of two fuzzy PD logic controller input linguistic variables E and DE , respectively. K_u is the output signal gain that fits the fuzzy PD logic controller output linguistic variable U to the corresponding control signal u of the BCD. When the control signal $u \geq +0.1$, the inflation valve opens; when the control signal $u \leq -0.1$, the deflation valve opens; and both valves are closed when $|u| < 0.1$. The inflation or deflation boundary of 0.1 is experimentally tuned to achieve optimum diver depth and diver velocity control at the expense of higher or lower air consumption. A boundary of 0.2 leads to oscillating diver depth control and lower air consumption, while a boundary of 0.05 significantly increases air consumption but does not improve the efficiency of diver depth control.

Figure 4 shows the input and output membership functions of the fuzzy PD logic controller and Table 1 shows the rule matrix for the corresponding FLCS. The position of the input membership functions is chosen to uniformly cover the entire definition space, and the position of the output membership functions is chosen to allow the fuzzy PD controller to behave nonlinearly according to the chosen fuzzy PD logic controller rules.

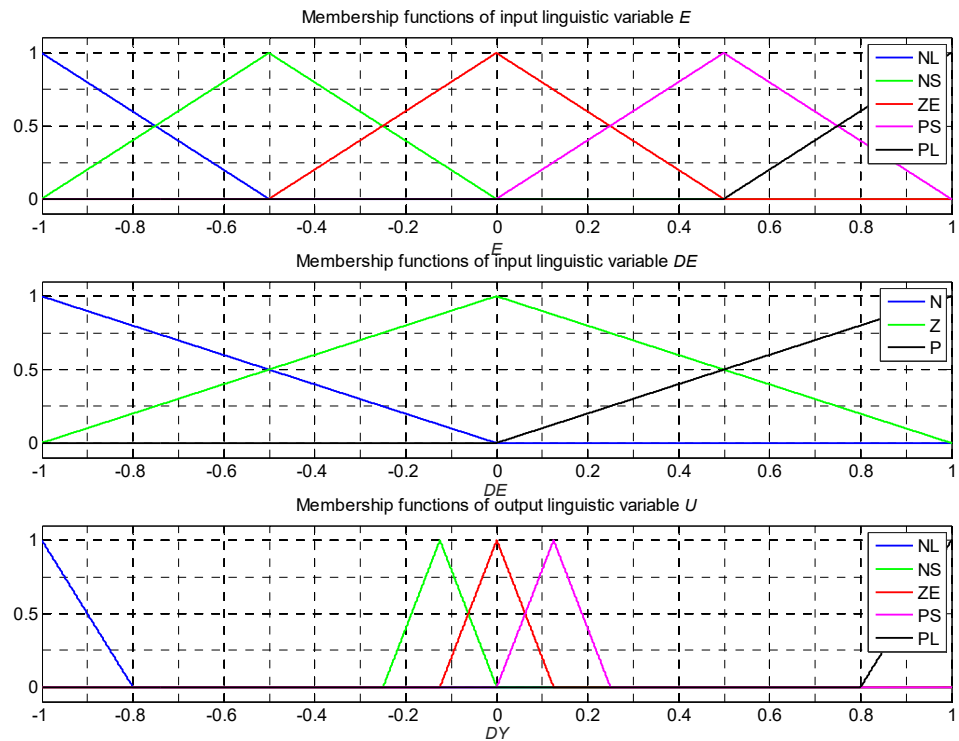


Figure 4. Fuzzy PD logic controller membership functions (N: negative, ZE: zero, P: positive, L: large, S: small).

Table 1. Rules matrix of the fuzzy PD logic controller.

		E					
		DE	NL	NS	ZE	PS	PL
DE	P	NL	ZE	PS	PL	PL	
	ZE	NL	NS	ZE	PS	PL	
	N	NL	NL	NS	ZE	PL	

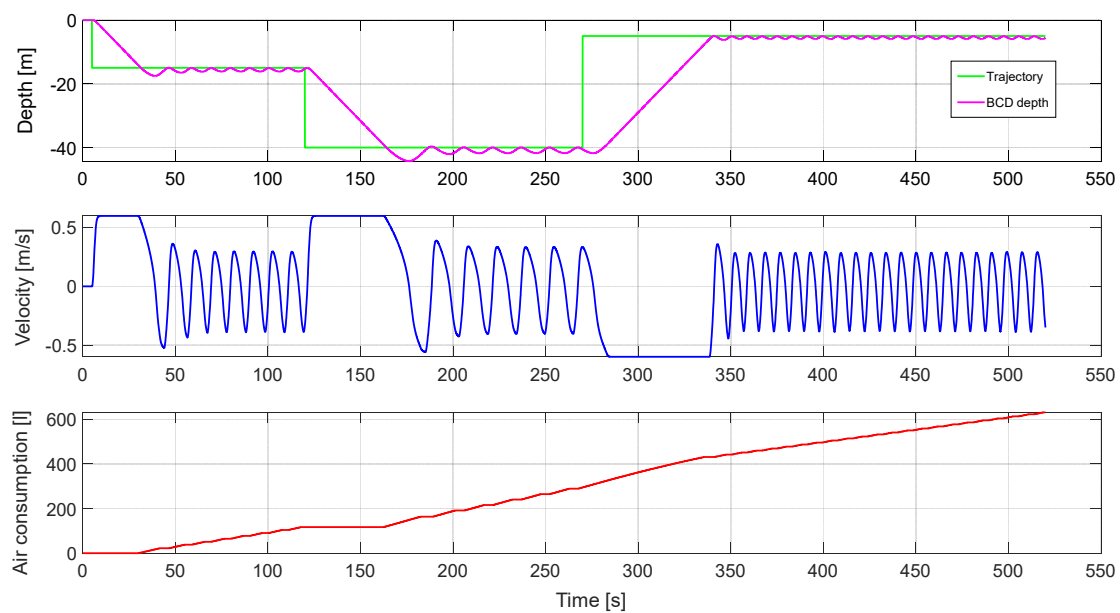


Figure 5. Control results obtained before optimization process.

All simulations were conducted in Matlab and Simulink on an existing nonlinear BCD mathematical model. The Mamdani inference mechanism was used and the FLCS input and output gains were determined by a human expert: $K_e = 0.1$, $K_{de} = 0.5$ and $K_u = 5.0$. This leads to oscillating depth control around the depth reference trajectory and an exceeding of diver safety requirements of ± 0.2 m/s at vertical diver speed. The air consumption of BCD is also very high (Figure 5).

4. Optimization-Aided Design of the FCLS

A differential evolution global optimum search algorithm [27–29] was used to design the optimal controller. Table 2 shows the five position FLCS parameters together with their corresponding range of values determined for the optimization procedure.

Table 2. Position FLCS parameters used in optimization design.

Symbol	Description	Value Range
K_e	Proportional gain of the position error	0.01–1.0
K_{de}	Proportional gain of the vertical velocity	0.01–1.0
K_u	Proportional gain of the control signal	0.01–5.0
NS	Center of the output NS membership function	−0.975–0.025
PS	Center of the output PS membership function	0.025–0.975

The objective function OF_1 , used in the optimization-aided design of the position FLCS combines the position control error e_p with the air consumption V_{air} :

$$OF_1 = \sqrt{\left(\int |e_p(t)| dt \right)^2 + (V_{air})^2}. \quad (11)$$

The values of the position FLCS parameters obtained by OF_1 objective function are shown in Table 3.

Table 3. Optimized parameters of position FLCS.

Symbol	Value
K_e	0.099
K_{de}	1.000
K_u	0.775
NS	−0.875
PS	0.025

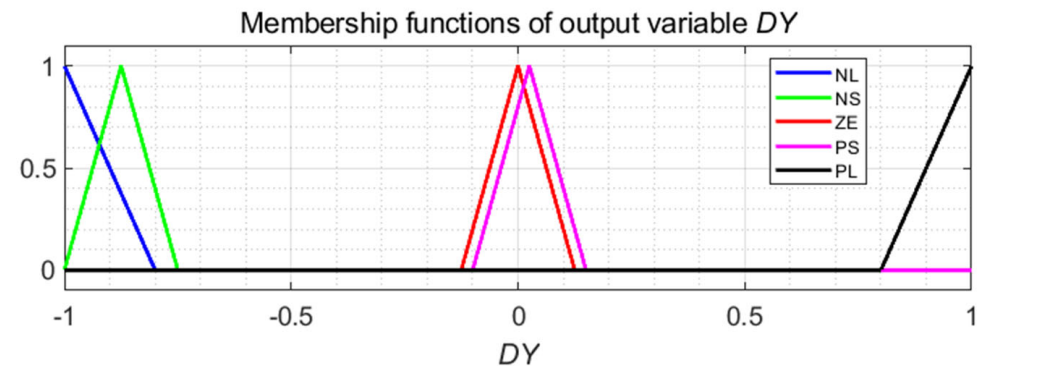


Figure 6. Position fuzzy PD logic controller membership functions of output variable DY after optimization with objective functions OF_1 (N: negative, ZE: zero, P: positive, L: large, S: small).

Figure 6 shows the position off the membership functions of the fuzzy PD logic controller for the output variable DY after applying the optimization procedure with

objective function OF1. We may notice how membership functions NS and PS are allocated after optimization with differential evolution global optimum search algorithm using the objective function OF1 in comparison to the initial locations shown in Figure 4.

Figure 7 shows the optimized position FLCS response. The results are far from expected. There are still oscillations around the reference depth, the vertical velocity exceeds the safety requirements, and the air consumption is very high.

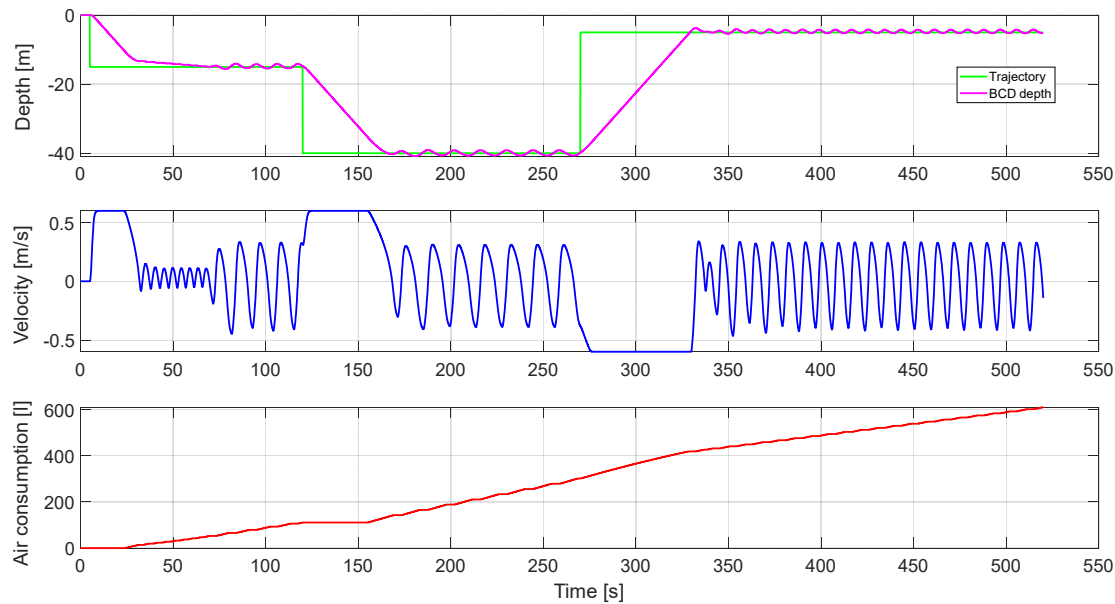


Figure 7. Control response obtained after the optimization process with the position FCLS.

To improve the simple position FLSC, the fuzzy PD controller was set as a velocity controller in the inner control loop and the linear proportional controller in the outer control loop, as proposed in our previous work [18], where a linear velocity PID controller is used instead of a velocity fuzzy PD controller.

Using the velocity error as the first input and the velocity error change over time as the second FLCS input leads to a velocity fuzzy PD control scheme, where the reference velocity signal is calculated by the linear P controller. In this case, the desired closed-loop response ideally behaves as a first order process with a time constant $1/K_v$ [30]. Figure 8 shows the setup of the velocity fuzzy PD control system.

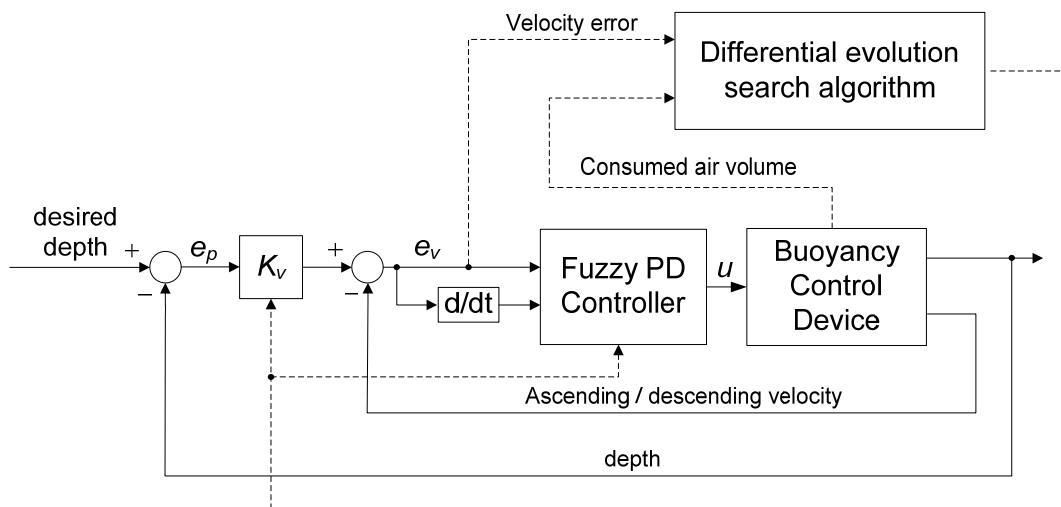


Figure 8. Velocity fuzzy PD control system setup for optimization-aided design.

For the velocity fuzzy PD controller, we used the same number of membership functions and the same set of rules as for the position fuzzy PD controller (Figures 3 and 4; Table 1). Table A2 in the Appendix A shows the six velocity FLCs parameters together with their corresponding range of values determined for the optimization process.

Three working regimes were tested. Objective function for the first working regime (OF_1) has been defined by Equation (11), where the position error e_p must be replaced by the velocity error e_v .

The second objective function (OF_2) for the second working regime reduces the significance of the achieved air consumption in the overall value of the objective function:

$$OF_2 = \sqrt{\left(\int |e_v(t)| dt\right)^2 + (0.5 \cdot V_{air})^2}, \quad (12)$$

and the third objective function (OF_3) for the third working regime consequently emphasizes the air consumption over the velocity control:

$$OF_3 = \sqrt{(0.5 \cdot \int |e_v(t)| dt)^2 + (V_{air})^2} \quad (13)$$

The velocity FLCs parameter values obtained with all three objective functions are shown in Table A3 in the Appendix A.

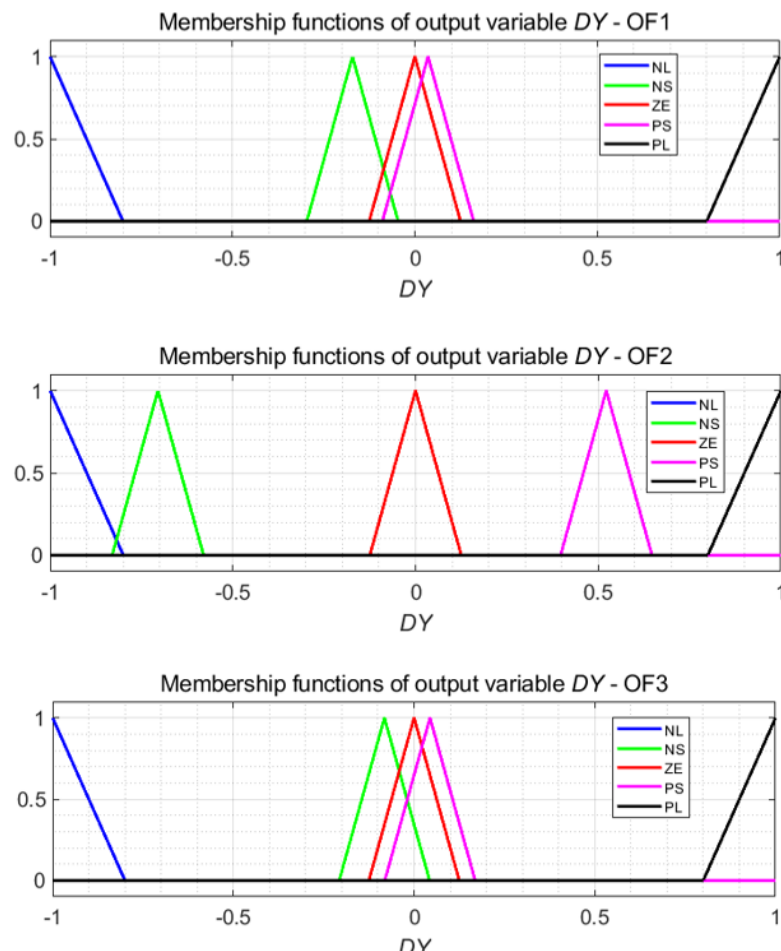


Figure 9. Velocity fuzzy PD logic controller membership functions of output variable DY after optimization with objective functions OF_1 , OF_2 and OF_3 (N: negative, ZE: zero, P: positive, L: large, S: small).

Figure 9 shows the velocity fuzzy PD logic controller membership functions of the output variable DY after applying the optimization procedure for all three working regimes. It can be noticed how the membership functions NS and PS are arranged after optimization with the differential evolution global optimum search algorithm using three different objective functions, OF1, OF2 and OF3.

Figure 10 shows the response of the optimized velocity FLCS for the resulting controller parameters for all three working regimes compared to the cascaded linear P-PID controller from [18].

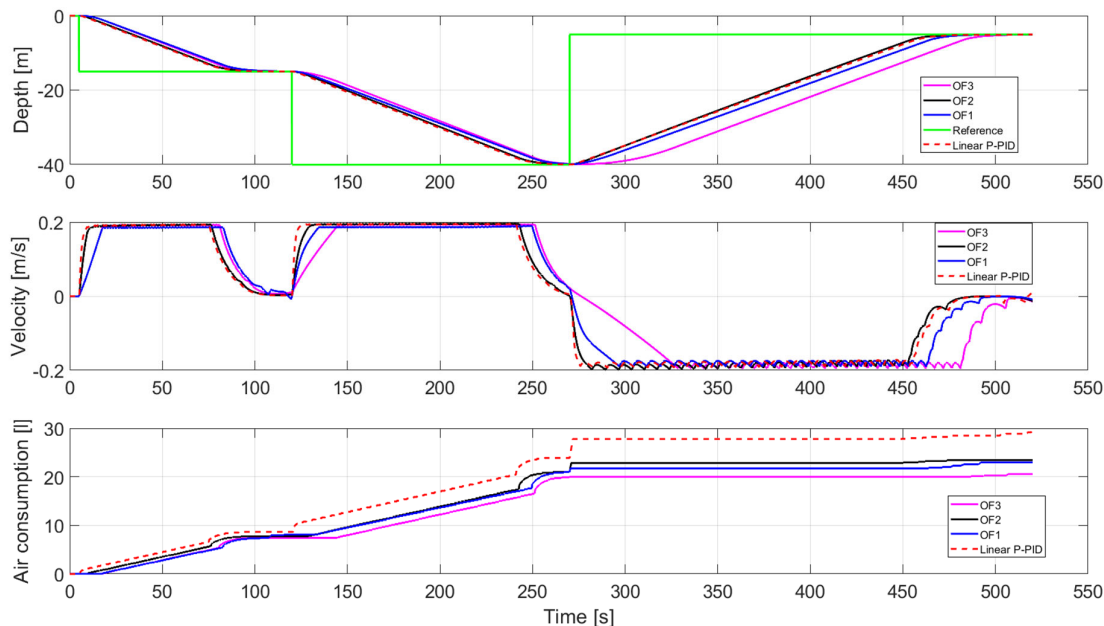


Figure 10. Velocity FLCS response obtained with all three objective functions compared to the cascaded linear P-PID controller.

All three working regimes achieved the desired velocity and depth control. All are within the vertical speed limits of ± 0.2 m/s and are therefore suitable for automatic BCD control. The second working regime achieved slightly better velocity and position control at the expense of higher air consumption. Because the third working regime met all the control requirements with lower final air consumption, it is the most favorable working regime for the automatic control of the BCD, even in comparison with the cascaded linear P-PID controller from [18].

Table 4 shows the values of the final air volume consumed V_{air} , the root mean squared velocity error $RMSE_v$ and the root mean squared position error $RMSE_p$ for all working regimes compared to the optimized cascaded linear P-PID controller.

Table 4. Final air consumption values, root mean squared velocity and position error.

	OF1	OF2	OF3	Cascaded P-PID
Consumed air (liters)	22.94	23.45	20.54	29.29
$RMSE_v$	0.0287	0.0206	0.0475	0.0287
$RMSE_p$	15.6935	14.8787	17.2962	14.8458

In real diving situations, a diver may pick up an object or drop a piece of equipment while diving. To validate the robustness of the velocity FLCS, we simulated a 2 kg increase in the diver's mass after 200 s of diving at a depth of 15 m. Figure 11 shows the control

response of the velocity FLCS with added mass (disturbance) after 200 s of diving for all three working regimes.

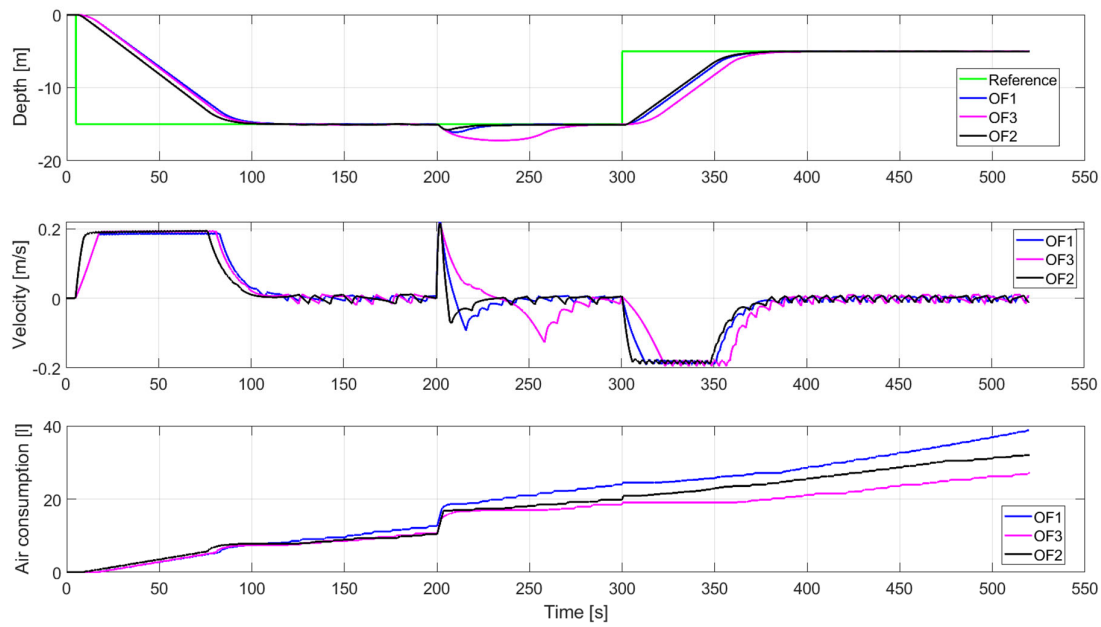


Figure 11. Velocity FLCS response obtained with all three objective functions after applying the disturbance.

After the applied disturbance, all three working regimes achieved a re-correction of the diver's depth. The first and second working regimes achieved slightly better depth correction at the expense of higher air consumption. The third working regime successfully corrected the diver depth with a lower final air consumption at the expense of a slower diver depth correction.

5. Conclusions

The automatic BCD controls the diver's depth and vertical velocity in combination with minimal air consumption. The vertical velocity of the BCD is potentially hazardous to the diver's health and should be limited to ± 0.2 m/s. The implemented fuzzy PD controller as a velocity FLCS was a cascade controller with an internal vertical velocity and an external depth control loop. The first setup of the velocity FLCS depended on the knowledge of the operator and did not need any corrections during the optimization process. For this reason, input-output signal gains corresponding to the normalized definition spaces of two fuzzy input linguistic variables and one fuzzy output linguistic variable were introduced. To take advantage of the use of FLCS nonlinearities in the optimization process, we also included the center of the two output membership functions (NS and PS). The optimization of the FLCS parameters was achieved using a differential evolution global optimum search algorithm for the three proposed working regimes and compared with a previously optimized cascaded linear P-PID controller. Similar control results were obtained with all three working regimes. The second working regime using the objective function OF_2 provides the best position and velocity control response on the expense of higher air consumption ($RMSE_p = 14,8787$, $RMSE_v = 0,0206$ and $V_{air} = 23,45$). The third working regime using the objective function OF_3 met all the control requirements with a lower final air consumption ($RMSE_p = 17,2962$, $RMSE_v = 0,0475$ and $V_{air} = 20,54$). It is the most favorable working regime for the automatic BCD. Compared to the optimized cascaded linear P-PID controller, the velocity FLCS achieved a 30% reduction in air consumption, which can be a major advantage in critical diving conditions. In the eventual application of the proposed velocity FLCS for real-time automatic BCD, only fine tuning of the already optimized parameters can be expected. The

fuzzy inference engine may be implemented as a static look-up table so time-consuming mathematical calculations may be avoided.

The dynamic effects of diver breathing, diving suit compression and different diver swimming modes are currently excluded in our model. Therefore, further research will focus on analyzing the effect of diver breathing and swimming on diver buoyancy by taking it into account with new control algorithms.

Author Contributions: Conceptualization, N.M., M.R. and M.G.; methodology, N.M., M.R. and M.G.; software N.M. and M.R.; validation, N.M. and M.R.; writing—original draft preparation, N.M.; writing—review and editing, N.M. and M.G.; visualization, N.M. and M.R.; supervision, N.M. and M.G. All authors have read and agreed to the published version of the manuscript.

Funding: The third author acknowledges the financial support from the Slovenian Research Agency (Research Core Funding No. P2-0028).

Institutional Review Board Statement: Not applicable.

Informed Consent Statement: Not applicable.

Conflicts of Interest: The authors declare no conflict of interest.

Appendix A

Table A1. Summary of symbolic parameters and simulation values.

Symbol	Description	Simulation Values
$z(t)$	diver's depth	
$z(0)$	initial diver's depth	0 m
$\dot{z}(t)$	velocity	
$\ddot{z}(t)$	acceleration	
c_d	drag coefficient	1.2
g	gravitational constant	9.81 m/s ²
m_d	diver's mass with equipment	85 kg
ρ_w	water density	1025 kg/m ³
V_{BCD}	air volume inside of buoyancy device	
$V_{BCD}(0)$	initial air volume inside of buoyancy device	0.005 m ³
V_d	diver's volume	0.08 m ³
S_{BCD}	buoyancy device frontal aerial surface	0.0283 m ²
S_d	diver's frontal aerial surface	0.2 m ²
p_z	surrounding ambient pressure	
p_0	atmospheric pressure at water level	97.574 k Pa
$T_z(t)$	absolute surrounding water temperature	304.5 K
$T_z(0)$	initial absolute water temperature	304.5 K
$T_{aI}(t)$	absolute inflated air temperature	304.5 K
$T_{aD}(t)$	absolute deflated air temperature	304.5 K
q_{VI}	added valve volume flow	
q_{VD}	deducted valve volume flow	
p_r	regulator pressure	857.426 kPa
R_a	gas constant for air	287
u	control signal	
κ	ratio of specific heat constants for dry air	1.4
A_I	add valve orifice surface	1.31 mm ²
α_I	add valve discharge coefficient	0.744
A_D	deduct valve orifice surface	11.34 mm ²
α_D	deduct valve discharge coefficient	0.68

Table A2. Velocity FLCS parameters used in optimization design.

Symbol	Description	Value Range
K_e	Proportional gain of the velocity error	0.01–5.0
K_{de}	Proportional gain of the velocity error derivative	0.01–10.0
K_u	Proportional gain of the control signal	0.01–10.0
NS	Center of the output NS membership function	-0.975–0.025
PS	Center of the output PS membership function	0.025–0.975
K_v	Proportional gain of position P controller	0.1–0.5

Table A3. Optimized velocity FLCS parameter values.

Controller Parameter	Value (OF1)	Value (OF2)	Value (OF3)
K_e	1.102	1.831	0.393
K_{de}	8.946	5.568	9.280
K_u	0.989	0.373	1.441
NS	-0.171	-0.705	-0.082
PS	0.036	0.522	0.044
K_v	0.100	0.100	0.100

References

- Bube, B.; Zanón, B.B.; Lara Palma, A.M.; Klocke, H. Wearable Devices in Diving: Scoping Review. *JMIR mHealth uHealth* **2022**, *10*, e35727. [[CrossRef](#)] [[PubMed](#)]
- Wiehr, F.; Höh, A.; Krüger, A. Towards a Wearable for Deep Water Blackout Prevention. In Proceedings of the Augmented Humans International Conference, Kaiserslautern, Germany, 16 March 2020; ACM: New York, NY, USA; pp. 1–3.
- Kuch, B.; Buttazzo, G.; Azzopardi, E.; Sayer, M.; Sieber, A. GPS Diving Computer for Underwater Tracking and Mapping. *Underw. Technol.* **2012**, *30*, 189–194. [[CrossRef](#)]
- Eun, S.J.; Kim, J.Y.; Lee, S.H. Development of Customized Diving Computer Based on Wearable Sensor for Marine Safety. *IEEE Access* **2019**, *7*, 17951–17957. [[CrossRef](#)]
- Allotta, B.; Pugi, L.; Gelli, J.; Lupia, M. Design and Fast Prototyping of a Wearable Safety Device for Divers. *IFAC-Pap.* **2016**, *49*, 547–552. [[CrossRef](#)]
- Huang, H.; Zhang, C.; Ding, W.; Zhu, X.; Sun, G.; Wang, H. Design of the Depth Controller for a Floating Ocean Seismograph. *J. Mar. Sci. Eng.* **2020**, *8*, 166. [[CrossRef](#)]
- Ranganathan, T.; Singh, V.; Thondiyath, A. Theoretical and Experimental Investigations on the Design of a Hybrid Depth Controller for a Standalone Variable Buoyancy System—VBuoy. *IEEE J. Ocean. Eng.* **2020**, *45*, 414–429. [[CrossRef](#)]
- Wang, J.; Wu, Z.; Dong, H.; Tan, M.; Yu, J. Development and Control of Underwater Gliding Robots: A Review. *IEEECAA J. Autom. Sin.* **2022**, *9*, 1543–1560. [[CrossRef](#)]
- Bonzon, D.; Sinclair, A.; Glez, C.; Webb, C. A Safe Automatic Buoyancy Control Device. U.S. Patent 13/432,063, 3 October 2013.
- Brecht, W.F., Jr. Buoyancy Control for Scuba Diving. U.S. Patent 3,487,647, 6 January 1970.
- Egan, M.P. Automatic Buoyancy Compensator with Electronic Vertical Motion. U.S. Patent 5,496,136, 5 March 1996.
- Tolksdorf, M.; Tolksdorf, T. Counterbalancing Device for Divers. U.S. Patent 5,482,40, 9 January 1996.
- Leonard, K.J.; Engel, J. Variable Buoyancy Apparatus for Controlling the Movement of an Object in Water. U.S. Patent 6,772,705, 10 August 2004.
- Dyer, R.J. Development of an Automatic Buoyancy Device for Application in Scuba Diving. Bachelor’s Thesis, Massachusetts Institute of Technology, Cambridge, MA, USA, 2001.
- Kuch, B.; Buttazzo, G.; Sieber, A. Bubble Model Based Decompression Algorithm Optimised for Implementation on a Low Power Microcontroller. *Underw. Technol.* **2011**, *29*, 195–202. [[CrossRef](#)]
- Valenko, D.; Mezgec, Z.; Pec, M.; Golob, M. A Diver’s Automatic Buoyancy Control Device and Its Prototype Development. *Mar. Technol. Soc. J.* **2013**, *47*, 16–26. [[CrossRef](#)]
- Valenko, D.; Mezgec, Z.; Pec, M.; Golob, M. Dynamic Model of Scuba Diver Buoyancy. *Ocean Eng.* **2016**, *117*, 188–198. [[CrossRef](#)]
- Rižnar, M.; Valenko, D.; Golob, M.; Muškinja, N. Optimized Diving Velocity and Depth Control for Diver’s Automatic Buoyancy Control Device. *Mar. Technol. Soc. J.* **2015**, *49*, 124–130. [[CrossRef](#)]

19. Mamdani, E.H. Application of Fuzzy Algorithms for Control of Simple Dynamic Plant. *Proc. IEEE* **1974**, *121*, 1585–1588. [[CrossRef](#)]
20. Ying, H. The Simplest Fuzzy Controllers Using Different Inference Methods Are Different Nonlinear Proportional-Integral Controllers with Variable Gains. *Automatica* **1993**, *29*, 1579–1589. [[CrossRef](#)]
21. Qiao, W.Z.; Mizumoto, M. PID Type Fuzzy Controller and Parameters Adaptive Method. *Fuzzy Sets Syst.* **1996**, *78*, 23–35. [[CrossRef](#)]
22. Lewis, F.L.; Liu, K. Towards a Paradigm for Fuzzy Logic Control. *Automatica* **1996**, *32*, 167–181. [[CrossRef](#)]
23. Mann, G.K.I.; Hu, B.-G.; Gosine, R.G. Analysis of Direct Action Fuzzy PID Controller Structures. *IEEE Trans. Syst. Man Cybern. Part B Cybern.* **1999**, *29*, 371–388. [[CrossRef](#)]
24. Arun, N.K.; Mohan, B.M. Modeling, Stability Analysis, and Computational Aspects of Some Simplest Nonlinear Fuzzy Two-Term Controllers Derived via Center of Area/Gravity Defuzzification. *ISA Trans.* **2017**, *70*, 16–29. [[CrossRef](#)]
25. Castillo, O.; Cortés-Antonio, P.; Melin, P.; Valdez, F. Type-2 Fuzzy Control for Line Following Using Line Detection Images. *J. Intell. Fuzzy Syst.* **2020**, *39*, 6089–6097. [[CrossRef](#)]
26. Sain, D.; Mohan, B.M. A Simple Approach to Mathematical Modelling of Integer Order and Fractional Order Fuzzy PID Controllers Using One-Dimensional Input Space and Their Experimental Realization. *J. Frankl. Inst.* **2021**, *358*, 3726–3756. [[CrossRef](#)]
27. Storn, R.; Price, K. Differential Evolution—A Simple and Efficient Heuristic for Global Optimization over Continuous Spaces. *J. Glob. Optim.* **1997**, *11*, 341–359. [[CrossRef](#)]
28. Ao, Y.; Chi, H. Experimental Study on Differential Evolution Strategies. In Proceedings of the 2009 IEEE WRI Global Congress on Intelligent Systems, Xiamen, China, 19–21 May 2009; pp. 19–24.
29. Li, G.; Liu, M. The Summary of Differential Evolution Algorithm and Its Improvements. In Proceedings of the 2010 IEEE 3rd International Conference on Advanced Computer Theory and Engineering (ICACTE), Chengdu, China, 20–22 August 2010; pp. 153–156.
30. Muškinja, N.; Rižnar, M. Optimized PID Position Control of a Nonlinear System Based on Correlating the Velocity with Position Error. *Math. Probl. Eng.* **2015**, *2015*, 796057. [[CrossRef](#)]

Disclaimer/Publisher’s Note: The statements, opinions and data contained in all publications are solely those of the individual author(s) and contributor(s) and not of MDPI and/or the editor(s). MDPI and/or the editor(s) disclaim responsibility for any injury to people or property resulting from any ideas, methods, instructions or products referred to in the content.